DE GRUYTER OPEN Open Phys. 2017; 15:1077–1085

Research Article

Mohammad Syuhaimi Ab-Rahman and Abdulhameed Almabrok Swedan*

Quadruple multi-wavelength conversion for access network scalability based on cross-phase modulation in an SOA-MZI

https://doi.org/10.1515/phys-2017-0136
Received Jul 14, 2017; accepted Oct 30, 2017

Abstract: The emergence of new services and data exchange applications has increased the demand for bandwidth among individuals and commercial business users at the access area. Thus, vendors of optical access networks should achieve a high-capacity system. This study demonstrates the performance of an integrated configuration of one to four multi-wavelength conversions at 10 Gb/s based on cross-phase modulation using semiconductor optical amplifier integrated with Mach–Zehnder interferometer. The Opti System simulation tool is used to simulate and demonstrate one to four wavelength conversions using one modulated wavelength and four probes of continuous wave sources. The wavelength converter processes are confirmed through investigation of the input and output characteristics, optical signal-to-noise ratio, conversion efficiency, and extinction ratio of new modulated channels after separation by demultiplexing. The outcomes of the proposed system using single channel indicate that the capacity can increase from 10 Gb/s to 50 Gb/s with a maximum number of access points increasing from 64 to 320 (each point with 156.25 Mb/s bandwidth). The splitting ratio of 1:16 provides each client with 625 Mb/s for the total number of 80 users. The Q-factor and bit error rate curves are investigated to confirm and validate the modified scheme and prove the system performance of the full topology of 25 km with 1/64 splitter. The outcomes are within the acceptable range to provide the system scalability.

Keywords: wavelength converter; cross-phase modulation; bandwidth demands; system performance

PACS: 42.65.Ky, 42.79.Nv, 42.82.Gw, 42.60.By

***Corresponding Author: Abdulhameed Almabrok Swedan:** Department of Electrical, Electronic & System Engineering, Faculty of Engineering and Built Environment, Universiti Kebangsaan Malaysia (UKM), 43600 Bangi, Selangor, Malaysia; Email: aswsw2002@yahoo.com

1 Introduction

Configurations of next-generation access networks are developing to adapt with emerging technology trends driven by various new technologies and applications, such as smartphones, the Internet of things, fifth-generation wireless systems, and video on demand. Thus, high-speed data rate and average bandwidth increasingly demand of access networks, thereby urging network providers and optical device designers to upgrade the components and integrate them with one another to obtain high-speed, high-capacity systems [1–3]. Optical semiconductor amplifiers (SOA's) are classified into two categories: amplification applications and data processing devices, which work in the saturation region as a nonlinear medium [4–10]. The use of SOA increases with the continuous emergence of new smart devices, which are multi-function component for a wide range of applications, such as optical switching, optical gates, and wavelength converters [11–15].

Wavelength conversion (WC) plays an essential role in addressing the problem and increasing the number of channels to achieve the requirements of high-speed, high-capacity systems. Several schemes have been employed to explain the operation of a wavelength converter using SOA; for example, in cross-gain modulation (XGM), the inverted data sequence is carried by the probe wavelength after the process [16–18]. The combined SOA can simply obtain non-inverted data and delayed interferometer consisting of delay loop, tunable coupler, and phase shifter. This configuration is implemented using one fiber at the input and output port [19, 20]. Meanwhile, cross-phase modulation (XPM) introduces the same data of pump and probe wavelengths demonstrated in [21]. The outers in [22] presented and simulated WC of high speed and 40 Gb/s data rate are based on XPM in an SOA-MZI architecture for

Mohammad Syuhaimi Ab-Rahman: Department of Electrical, Electronic & System Engineering, Faculty of Engineering and Built Environment, Universiti Kebangsaan Malaysia (UKM), 43600 Bangi, Selangor, Malaysia

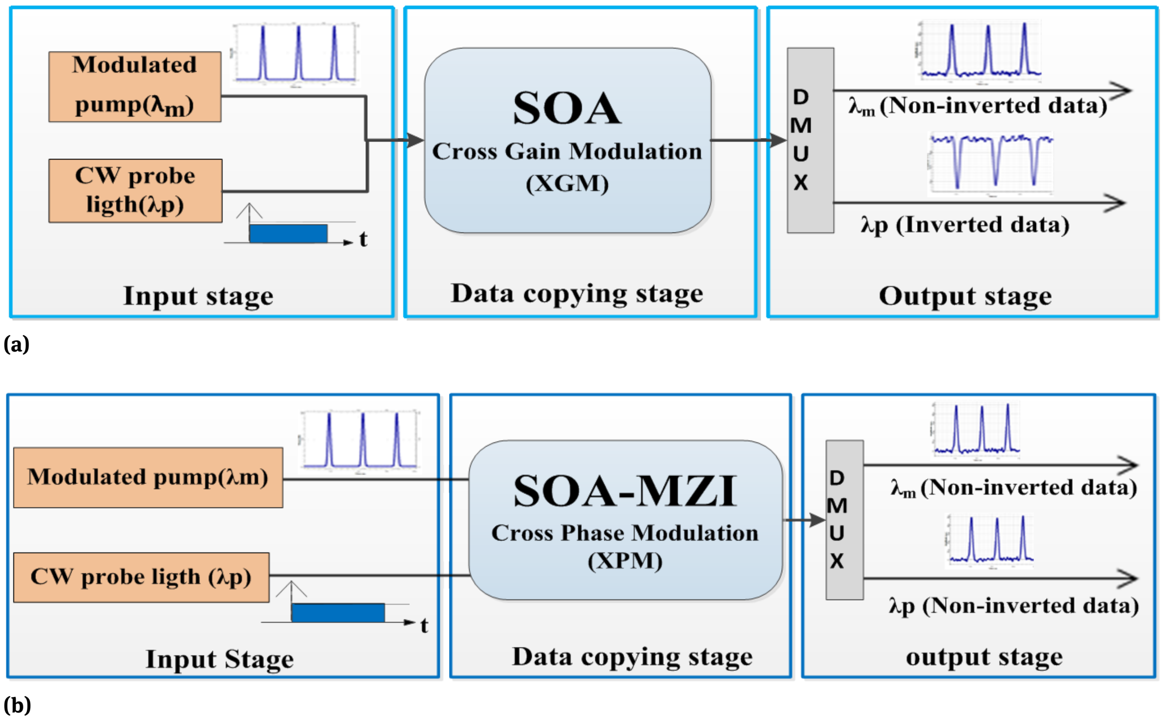

Figure 1: Basic wavelength conversion configuration: (a) XGM, (b) XPM

up- and down-conversion of WDM networks. Four-wave mixing (FWM) presents low conversion efficiency (CE). For example, Awang et al. obtained a CE of -47 dB; however, the method can offer required power for only a few applications [23–27]. Some studies have considered the wavelength converter in optical network unit (ONU) for upstream broadcast [28]. These different methodologies enabled to increase the number of channels and decreased the number of high-cost light sources, thereby extending the optical link reach of optical networks.

Multi-wavelength conversion (MWC) copies data from one pump wavelength to many continuous-wave (CW) probes of several wavelengths at the central office. Consequently, the data rate (Gb/s) of the modulated input signal can be duplicated; then, the data sequence is delivered at the output wavelengths with the same data rate as the original pump [29–31]. Unfortunately, these configurations need to use erbium-doped fiber amplifier (EDFA). The researchers at UKM examined and demonstrated the possibility to apply (one to two) wavelength conversion at the ONU after 20 and 25 km XGM and XPM, respectively. The basic configurations of this method are shown in Figure 1. First, the authors clarified the importance of SOA position when used as a data processing device. The model can be implemented to achieve MWC based on XGM-SOA at a bit rate of 10 Gb/s for one pump of 1541 nm; this structure can copy the inverted data to the probes at 1554 and 1558 nm. The influence of pump power on the system performance was evaluated and demonstrated at different positions of SOA. The results showed a splitting ratio of 1:64 for the new and old channels at a pump power of 3 dBm. The SOA-MZI configuration generating the same data sequences (non-inverted) based on 1 to 2 XPM at the ONU achieves a splitting ratio of 1:64 for all channels. This finding was verified and investigated, and different data format was tested for up and down conversion at specified settings of design parameters. The method proves that the wavelengths for up-conversion are 1540, 1541, 1542, 1551, 1552, and 1553 nm; those for down conversion are 1559, 1561, 1562, and 1565 nm. Applying the configuration on the network with ten channels can upgrade the system capacity to 300 Gb/s and the number of users to 1920.

In conclusion, the structure offers the possibility to achieve up and down conversion and is suitable to distribute a splitting ratio of 1:64 per wavelength. The configuration uses one pump signal (λm) with 10 Gb/s speed and two probes (λp) using CW light sources. The method can work in return and non-return (RZ and NRZ) formats, and the structure can increase the number of users of one channel system from 64 to 192 with 156.25 Gb/s bandwidth [32, 33].

The proposal mentioned above uses two CW sources as a probe, thereby limiting the total number of access points that can be generated. Therefore, the massive de-

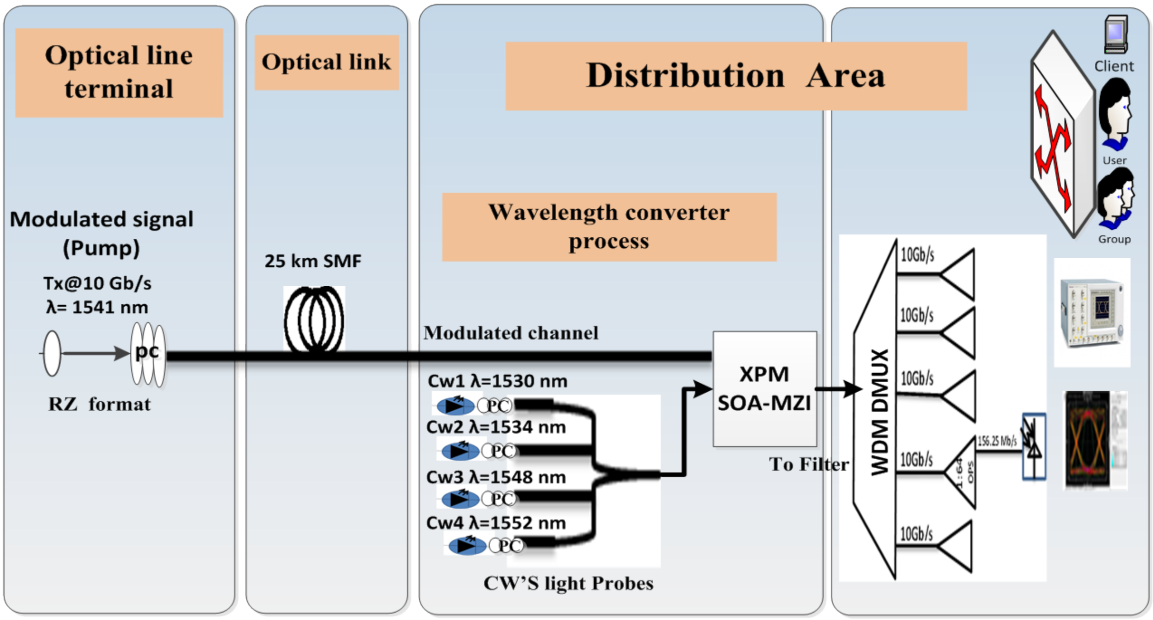

Figure 2: System configuration of MWC (one to four XPM based on SOA-MZI)

Table 1: Parameters used in this study based on those used in (32, 33)

symbol	parameter	parameter value				
		1 to 2 XGM (32)	1 to 2 XPM (33)‘impress’		1 to 4 XPM (this work)	
-	Bit rate	10 Gb/s	10 Gb/s		10 Gb/s	
-	Data format	Gaussian signal	Gaussian signal, NRZ, and RZ		RZ	
λ_{pump}	pump wavelength	1541 nm	Up-conversion of 1541–1553 nm Down-conversion of 1561–1562 nm		1541 nm	
P_{pump}	Pump power range	−6 to 3 dBm	5 to −3 dBm		3 to −1 dB/m	
λ_{probe}	Probe wavelength	1554 nm /1558 nm	1556 nm/1558 nm		Down-conversion of 1530–1534 nm Up-conversion of 1548–1552 nm	
P_{probe}	Probes power	0 dBm	3 to −5 dBm		0 to −5 dB/m	
			SOA-MZI		**SOA-MZI**	
			SOA1	**SOA1**	**SOA1**	**SOA2**
Ic	Bais current	200 mA	300 mA	250 mA	350 mA	250 mA
L	Active region length	600 µm	600 µm	600 µm	300 µm	300 µm
Γ	Confinement factor	0.45	0.45	0.45	0.45	0.45

mands of average download bandwidth for smart application are inadequate, and a large number of CW sources should be installed to provide a large number of access points and satisfy user's requirements. For this purpose, the configuration of one to four MWC based on XPM is demonstrated and verified in the current study.

This study demonstrates the possibility to upgrade current access networks by integrating SOA and MZI structure based on the XPM property at the ONU side, and utilize this feature to improve system capacity and the number of clients. The rest of the paper is organized as follows. Section 2 illustrates the parts of the system configuration transmitter (Tx), link, multi-wavelength converter block, and receiver (Rx), as well as the combined configuration principle of one to four MWC based on SOA-MZI. Section 3 discusses the mathematical background with the parameters for simulation tabulated in Table 1. Part 4 focuses on the results and outcomes of the scheme. In particular, the power spectrum and noise after XPM are displayed, the wavelength converter process is analyzed, and the performance is verified. Finally, Section 5 elaborates the conclusions of the study.

2 System methodology and configuration

This work aims to establish an efficient and reliable configuration network that provides a large number of access points and increased system capacity. For this purpose, one to four MWC based on XPM using semiconductor optical amplifier integrated with Mach–Zehnder interferometers (SOA-MZI) is examined and simulated. The Opti System simulation tool is used to confirm the wavelength converter. The methodology of this research involves two parts. In the first part, wavelength converter process is verified by analyzing the optical signal-to-noise ratio (OSNR), (CE), and extinction ratio (ER) of converted signals. In the second part, the bit error rate and Q-factor curves are measured to evaluate the system performance for the end customers for converted probes and pump channel. This architecture provides vendors the ability to develop the existing networks by improving bandwidth and increasing the number of users.

The recommended simultaneous one to four XPM wavelength converters at 10 Gb/s based on the SOA-MZI structure using a return-to-zero (RZ) data format is schematically shown in Figure 2. The system comprises optical line terminal (OLT) transmitter side, 25 km single-mode fiber (SMF), wavelength conversion operation block, distribution side de-multiplexing, and an optical splitter. The modulated pump light of 1541 nm carrying 10 Gb/s RZ data is implemented with optical polarization control to achieve parallel polarization. The pump signal transmits along 25 km SMF as presented in Figure 1, and then injects into the upper arm of the SOA-MZI configuration. In the multi-wavelength converter, the four CW lights at carefully chosen probe wavelengths from 1530 to 1534 nm for down-conversion and from 1548 to 1552 nm for up-conversion are used. The spacing between the pump and probes and that between probes should be appropriately set to avoid the FWM matching. In this configuration, the spacing between the pump and probes are adjusted to 7 nm to reduce crosstalk, while each couple of probes is spaced by 4 nm. Then, the four probes are combined using a power combiner in 4:1 structure. After that injected into the upper and lower arms of SOA-MZI through an optical coupler. The WC device called SOA-MZI integrates two SOA connected in series with the optical phase shift to control the XPM operation. The XPM is completed, and the four probes are impacted by modulated pump frequency processes inside the SOA-MZI structure, thereby enabling copying of the same pump data to all probes. Subsequently, the output passes through the wavelength division demultiplexer (WDM DMUX) to separate wavelengths. Next to that, all wavelength channels are inserted into the optical splitter in 1/N distribution to increase scalability. Finally, the PIN receiver is used to detect the signal, and the performance for each user is demonstrated using the bit error rate analyzer.

3 Theoretical background

The main contribution of this work is the SOA-MZI structure. The steady-state numerical model presented by Connelly [34] is considered to govern the input and output behavior of the architecture. By numerical simulation of a wideband steady-state model, the proposed one to four WCs based on XPM is stimulatingly realized using OptiSystem software. In this model, the changes in carrier density along the amplifier will affect all input signals (pump and probes); thus, nonlinearities can occur on the SOA. The set of coupled differential equations, which distinguish the interaction among the input signals, amplified spontaneous emission and carrier density were used in this model.

The signal field is obtained using the travelling wave equation below:

$$\frac{dE^{+}_{s_K}(z)}{dz} = \left(-j\beta_k + \frac{1}{2}\left(\Gamma g_m\left(\nu_k, n\right) - \alpha(n)\right)\right) E^{+}_{s_K}(z) \quad (1)$$

$$\frac{dE^{-}_{s_K}(z)}{dz} = \left(j\beta_k - \frac{1}{2}\left(\Gamma g_m\left(\nu_k, n\right) - \alpha(n)\right)\right) E^{-}_{s_K}(z) \quad (2)$$

Where E^{+}_{s} and E^{-}_{s} Positive and negative field component, β_k is the kth signal propagation coefficient, α material loss coefficient, g_m Optical gain coefficient at frequency ν, Γ optical mode confinement factor,n conduction band carrier density.

Consequently, the amount of spontaneous emission photon rates N^{+}_{j} and N^{-}_{j} noise generated through the SOA is computed as follows:

$$\frac{dN^{+}_{j}(z)}{dz} = \left(\Gamma g_m\left(\nu_j, n\right) - \alpha(n)\right) N^{+}_{j} + R_{SP}\left(\nu_j, n\right) \quad (3)$$

$$\frac{dN^{-}_{j}(z)}{dz} = -\left(\Gamma g_m\left(\nu_j, n\right) - \alpha(n)\right) N^{-}_{j} + R_{SP}\left(\nu_j, n\right) \quad (4)$$

Where $R_{SP}\left(\nu_j, n\right)$ spontaneously emitted noise coupled into N^{+}_{j} or N^{-}_{j}.

In the steady-state numerical model, the amplifier is divided into a number of segments $i = 1$ to N_z. The signal fields and spontaneous emission photon rates are estimated at the section boundaries, while the carrier density is investigated at the center of the section. The variation in carrier density (n) (m^3) at position z as a function of time is described using the following rate equation:

$$\frac{dn(z)}{dt} = \frac{I}{edLW} - R(n(z)) - \frac{\Gamma}{dW}\left\{\sum_{k=1}^{N_s} g_m(v_k, n(z))\left(Ns_k^+(z) + Ns_k^-(z)\right)\right\} - \frac{2\Gamma}{dW}\left\{\sum_{j=0}^{N_m-1} g_m(v_j, n(z))\, k_j\left[N_j^+(z) + N_j^-(z)\right]\right\} \quad (5)$$

where I bias current, $R(n(z))$ recombination rate, (d,w and L) active region thickness, width, and length respectively, e electron charge.

Equation (5) consists of four terms. The first part represents the addition of carriers to the active region from bias current; the second is recombination rate term; 2nd and 3rd portion on the RHS. Of Eq. (5) represent radiative recombination of carriers due to the amplified signal and ASE noise.

The full model expectations, parameters, and examination are explained in [34, 35].

OSNR, ER, and CE are deliberated to investigate and verify the configuration of the conversion operation.

1. Optical signal to noise ratio (OSNR) [36]

$$OSNR_{out} = \frac{p_{out}}{\sigma^2} \quad (6)$$

2. Extinction ratio (ER) [37]

$$ER_{out} = 10\left(\frac{P^1_{Pout}}{P^0_{Pout}}\right) \quad (7)$$

3. Conversion efficiency (CE) [38]

$$\eta = \log\frac{P_{out}(\lambda_{conv})}{P_{in}(\lambda_{pump})} \quad (8)$$

In the equations, P_{out} is the CW output power, σ is the noise variance, and P_{in} is the pump input signal power. Table 1 summarizes the parameters used in this work.

4 Results and discussion

The structure of the proposed scheme established for the setup is presented in Figure 2. The outcomes tested for the adjusted parameters of SOA are shown in Table 1. The two SOAs are optimized for up- and down-conversion to improve the power of converted signals. The static performance of the SOA-MZI for original and converted channels has been measured. In this work, one to four MWC governed by XPM characteristic based on integrated SOA-MZI configuration is verified and investigated. The system consists of one pump signal of 1541 nm with RZ data format, as well as four CW probes at 1530–1534 nm up-conversion and 1548–1552 nm down-conversion. The optimal condition of SOA-MZI is set up to achieve interface between pump and probe powers with device parameters on the output side. Figures 3(a) and (b) illustrate the capture of the power spectrum and noise after the XPM operation, respectively. Figure 3(a) displays good power levels achieving approximately 3 dBm for all probe wavelengths at the SOA output. The amplitude of FWM components has a lower power level of around 30 dBm than CW's power. Figure 3(b) describes the ASE noise profile with a power level of approximately −52 dBm, which clarifies the range of acceptable noise for this proposal.

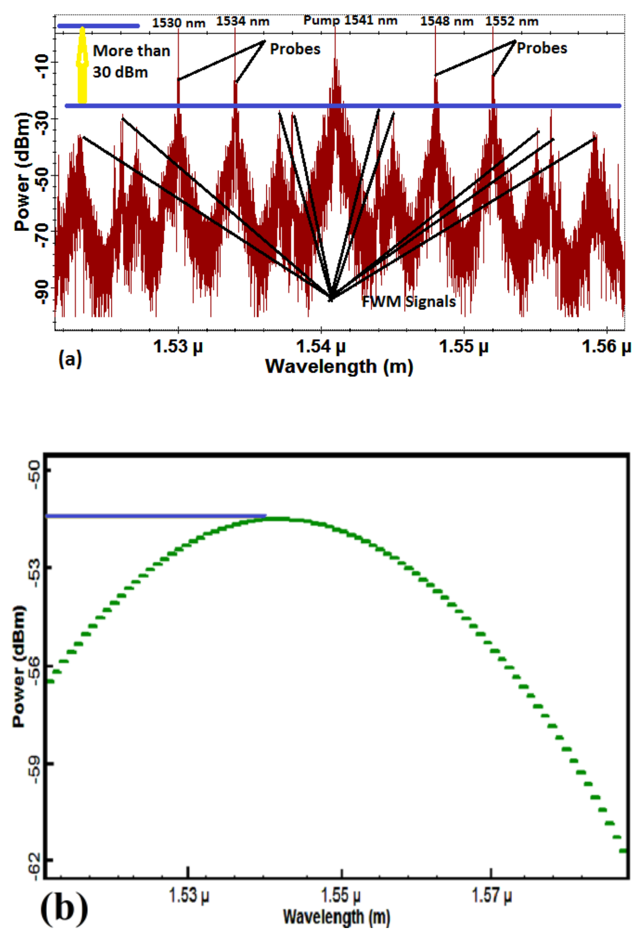

Figure 3: SOA-MZI output spectrum after the XPM operation: (a) multiwavelength spectra; (b) ASE spectra

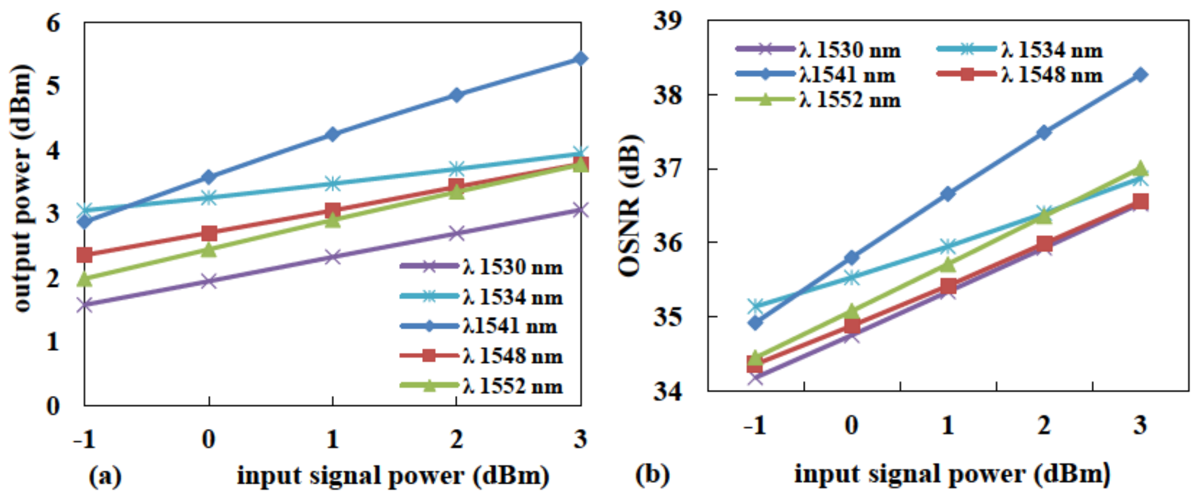

Figure 4: SOA-MZI characterization of basic and converted channels: (a) output power of various input power changes; (b) dependency of OSNR on input power

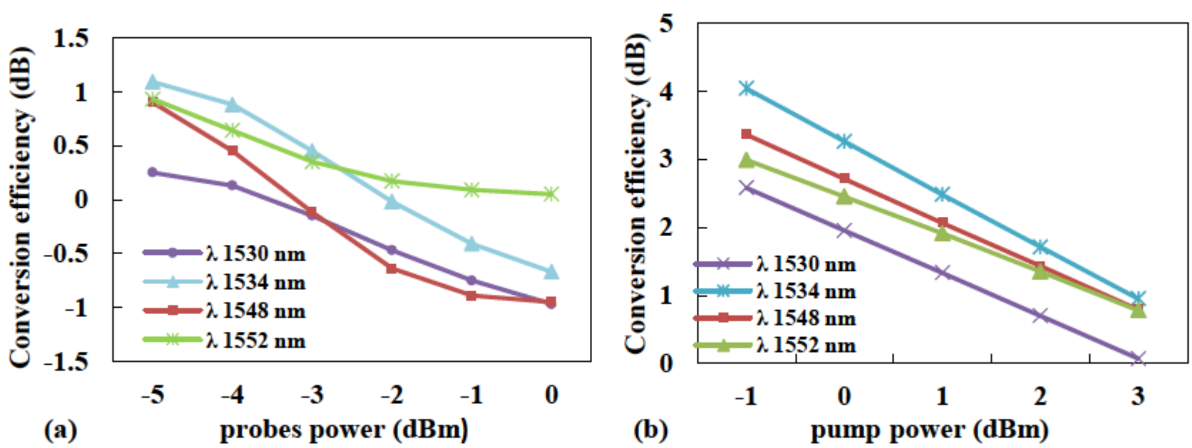

Figure 5: CE of converted wavelengths: (a) fixed pump power; (b) fixed probe power

4.1 Analysis of WC process

The XPM process is investigated by analyzing the behavior of wavelengths after filtering in terms of power change effect on different parameters as described below.

4.1.1 Influence of input power on output power and OSNR

Figure 4(a) illustrates the variation in output powers for basic and converted channels; this change depends on the input power of a fixed probe power of -5 dBm. The output power increases with the rise in the input power; high output power values for all frequencies at 3 dBm signal power means a high value of the basic wavelength. The effects of input optical pump on OSNR plotted in Figure 4(b) show that the increase in input power improves the OSNR of the output power. Moreover, the values of OSNR fluctuates between 34.14 dB minimum at −1 dBm for 1530 nm and 38.27 dB maximum at 3 dBm for 1541 nm. All values are in good agreement.

4.2 Influence of input pump power on CE

The CE of converted channels 1530, 1534, 1548, and 1552 nm are calculated in two criteria, as shown in Figures 5 (a) and (b). First, at 3 dBm pump power when the probe power is changed from −5 dBm to 0 dBm, the second varying pump power is between −1 and 3 dBm with sitting total probe power at −5 dBm. From Figures 5 (a) and (b), the CE declines with the increase in the input power, this is in agreement with previous results in the literature. Moreover, the value of CE is more than 0 dBm for all wavelengths at 3

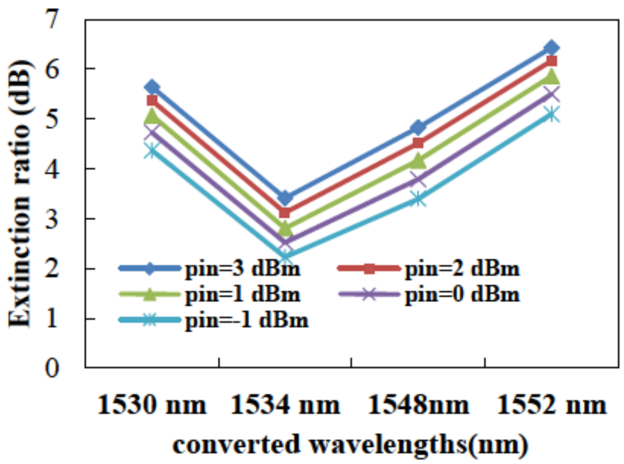

Figure 6: ER as a function of converted wavelengths for different pump power levels

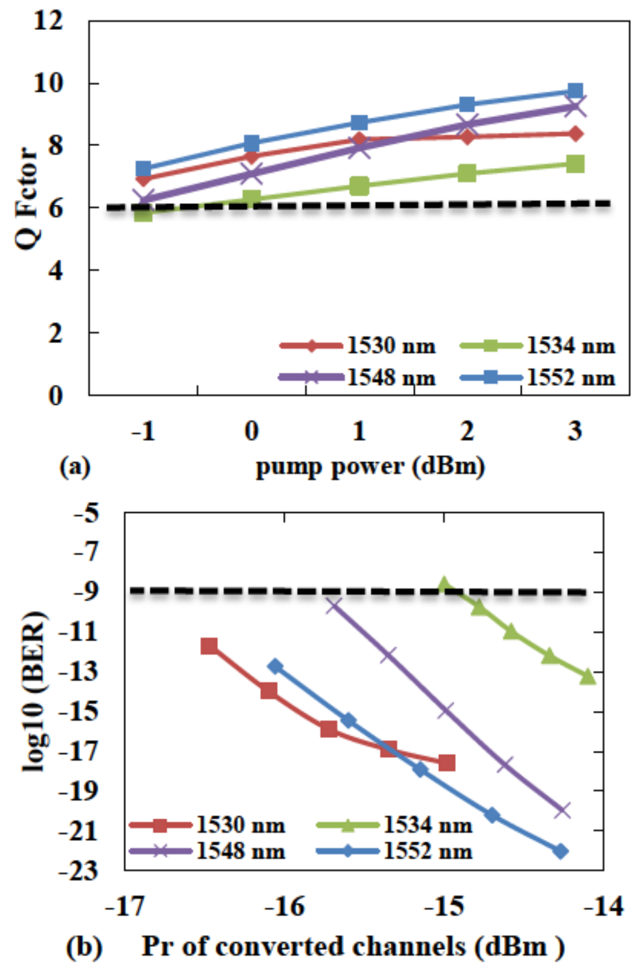

Figure 7: Performance of de-multiplexed channels Q-performance (a) as a function of the input pump signal and BER (b) as a function of received powers

dBm pump and −5 dBm probes and is thus considered an acceptable value for XPM schemes.

4.2.1 Influence of probe wavelength on ER

The results of this study show that the ER measurement of up and down-converted channels for various values of pump power is between 3 and −1 dBm. From the graph below, ER is proportional to pump power and obtains the best value at 3 dBm. The values of ER for 1552 nm are better than those for other channels. Meanwhile, the values for 1534 nm obtain lower values than those for other frequencies.

4.3 Performance of the proposed system

The analysis of the up- and down-converted wavelengths at end clients using an optical splitter (1:64) is verified through Q-factor and BER measurement of the outcomes as illustrated in Figures 7(a) and (b) in order to demonstrate the overall system performance of the scheme.

Figures 7(a) and (b) provide the results obtained from the Q-factor analysis for converted channels at various pump powers and BER curves. In all cases, the wavelengths 1530, 1534, 1548, and 1552 nm obtain an acceptable result for all values of pump power except for one value of 1534 nm that records 5.84. Furthermore, the Q-factor values of 1552 nm are highest and fluctuated between 7.26 and 9.74.

The system can be implemented at the ONU to offer one to four WC based on XPM after 25 km SMF, and the output power of each CW can be split into 1:64 clients. The findings of this research provide insights for increasing the optical channel capacity four times from 64 users with 156.25 Mb/s to 320 users at the same download speed. For scalability, the system with 10 pump wavelength (each occupied with four CWs) can implement the proposed system to provide the required bandwidth for 3200 customers. Moreover, the scheme offers the possibility to serve users with a broad range of bandwidths using different splitting ratios. Then, the configuration should be implemented with 10 channels to obtain the total system capacity of 500 Gb/s, thereby providing a simple scalability system. The topology offers many advantages, such as satisfying the coexistence with existing standards, the absence of EDFA, easy upgrading, and brown network scenario using the same infrastructure, which contributes the cost-effectiveness of a system and the capability to satisfy users' requirements of bandwidth. The possible options of

Table 2: Users' downstream bandwidth possibility of the proposed system compared with 1 to 2 XPM [31]

				Basic optical channel	1 to 2 XPM [31]'in press'	1 to 4 XPM (This work)
Total System Capacity				10 Gb/s	30 Gb/s	50 Gb/s
Point to point			Bandwidth	10 Gb/s	3 to 3 10 Gb/s	5 to 5 10 Gb/s
			No.users	1	3	5
Point to multi-point	**Splitting ratio**	1:8	Bandwidth	1.25 Gb/s	1.25 Gb/s	1.25 Gb/s
			No.users	8	24	40
		1:16	Bandwidth	625 Mb/s	625 Mb/s	625 Mb/s
			No.users	16	48	80
		1:32	Bandwidth	312.5 Mb/s	312.5Mb/s	312.5Mb/s
			No.users	32	96	160
		1:64	Bandwidth	156.25 Mb/s	156.25 Mb/s	156.25 Mb/s
			No.users	64	192	320

downstream bandwidth based on the splitting ratio for one channel system are summarized in Table 2.

Significant arguments and recommended future works are as follows:

1. The SOA device should be arranged to work in a saturation region by adjusting the total input power (modulated pump and CW probes) injected into the amplifier.
2. The sensitivity of the device to FWM is attributed to two factors: one is the space between the pump and probes, and the other is the space among the CW's lasers, and the number of CW's lasers used. These factors should be accordingly considered.
3. The model for standard PON's using wavelengths of 1490 and 1550 nm for downstream will be a good challenge (under progress).
4. An additional number of CW's should be applied to achieve a large-capacity system.

5 Conclusion

This study demonstrates the possibility to implement quadruple WC configuration at ONU. In this structure, converting modulated RZ data at 10 Gbit/s for 1541 nm to 4 CWs depends on the nonlinear property (XPM) of SOA. The investigation of converted channels shows that the scheme can copy data from the pump wavelength to all four probe wavelengths for the considered design. Also, the performance of output power of the converted channels can be attributed to 1:64 splitter with suitable values of Q-factor and BER. Therefore, the architecture can provide an appropriate upgrade of wavelength division multiplexing networks. Further studies should be carried out to validate and optimize the topology.

Conflict of Interests: The authors declare no conflict of interests.

Acknowledgement: This work was supported by the Faculty of Engineering and Built Environment, Universiti Kebangsaan Malaysia.

References

[1] Chen H.Y., Wei C.C., Lu I.C., Chu H.H., Chen Y.C., Chen J., High-Capacity and High-Loss-Budget OFDM Long-Reach PON without an Optical Amplifier, J.Opt. Commun. Netw, 2015, 7(1), A59-A65.

[2] Maier M., The escape of Sisyphus or what "Post NG-PON2" should do apart from never ending capacity upgrades, Photonics, 2014, 1(1), 47-66.

[3] Li B., Feng Z., Tang M., Xu Z., Fu S., Wu Q., Deng L., Tong W., Liu S., Shum P.P., Experimental demonstration of large capacity WSDM optical access network with multicore fibers and advanced modulation formats, Opti. Expr., 2015, 23(9),10997-11006.

[4] Qin J., Lu G.W., Sakamoto T., Akahane K., Yamamoto N., Wang D., Ji Y., Simultaneous multichannel wavelength multicasting and XOR logic gate multicasting for three DPSK signals based on four-wave mixing in quantum-dot semiconductor optical amplifier, Opti. expr, 2014, 22(24), 29413-29423.

[5] Raz O., Semiconductor optical amplifiers and their application for all optical wavelength conversion, In: Urquhart P., Advances in Optical Amplifiers, Intech, 2011

[6] Matsuura M., Calabretta N., Raz O., Dorren H.J., Multichannel wavelength conversion of 50-Gbit/s NRZ-DQPSK signals using a quantum-dot semiconductor optical amplifier, Opti. Expr., 2011, 19(26), B560-B566.

[7] Hui Z.Q., All-optical 1-to-8 wavelength multicasting at 20 Gbit/s exploiting self-phase modulation in dispersion flattened highly

nonlinear photonic crystal fiber, Sci. World J., 2014.
[8] Zajnulina M., Lingnau B., Ludge K., Four-wave mixing in quantum dot semiconductor optical amplifiers: a detailed analysis of the nonlinear effects,IEEE Jour. Selec. Top.Quan. Electr, 2017, 23(6), 1-12.
[9] Salleh M.S., Yusof Z. M., Supa'at A.S.M., Idrus S.M., Broadcasting, and Multicasting in All-Optical Packets Routing TWDM PON System Architecture, IJCNWC, 2012, 2(6), 749-755.
[10] Premaratne M., Agrawal G.P., Light propagation in gain media: optical amplifiers, 1st ed, Cambridge University Press, 2011
[11] Cheng Q., Ding M.,Wonfor A., Wei J., Penty R.V., White I.H., The feasibility of building a 64× 64 port count SOA-based optical switch, Sep 22, 2015, International Conference on Photonics in Switch- ing, 2015, 199-201.
[12] Sahafi M., Rostami A., Sahafi A., All-optical high speed logic gates using SOA, Opti. Communi., 2012, 285(9), 2289-2292.
[13] Singh S., Singh S., Badraoui N., Berceli T., Alomainy A., Design and analysis of all-optical up-and down-wavelength con- verter based on FWM of SOA-MZI for 60 Gbps RZ data signal, Phot. Netw. Communi., 2017,34(2), 288-297.
[14] Gong J., Xu J., Luo M., Li X., Qiu Y., Yang Q., Zhang X., Yu S., Alloptical wavelength conversion for mode division multiplexed superchannels, Opti. expr., 2016, 24(8), 8926-8939.
[15] Eramo V., Cianfrani A., Germoni A., Miucci E., Listanti M., SOA-based Optical Packet Switching Architectures, INTECH, 2012.
[16] Tingting P., Peili L., Shijie H., Zanshan Z., Multi-wavelength converter exploiting cross-gain modulation in SFRL, Asia Communications and Photonics Conference and Exhibition, (13–16 November 2011, Shanghai, China), 2011, 830-822.
[17] Yeh C.H., Chow C.W., Wu Y.F., Shih F.Y., Utilizing 1.2 GHz bandwidth reflective semiconductor optical amplifier for 1.25–10 Gbit/s for colourless and cooler-less wavelength conversion, Opti. Quant. Electr., 2013, 45(11),1223-1227.
[18] Salleh M.S., Manaf Z.A., Kadir Z.A., Yusof Z.M., Supa'at A.S., Idrus S.M., Khairi K., Simulation on physical performance of TWDM PON system architecture using multicasting XGM, (ICP), (Oct 1, 2012, InPhotonics), IEEE 3rd International Conference, 2012, 46-50.
[19] Leuthold J., Joyner C.H., Mikkelsen B., Raybon G., Pleumeekers J.L., Miller B.I., Dreyer K., Burrus C.A., 100 Gbit/s all-optical wavelength conversion with integrated SOA delayed-interference configuration, Electr. Lett., 2000, 36(13), 1129-1130.
[20] Tang X., Kim N.Y., Cartledge J.C., Noise transfer characteristics in a semiconductor optical amplifier with application to wavelength conversion based on a delay interferometer, Jour. Ligh. Tech., 2008, 26(12), 1715-1721.
[21] Khalil S., Ali R., Ghasem R., Mahboubed D., All-optical Semiconductor Optical Amplifiers Using Quantum Dots (Optical Pumping), Some Advanced Functionalities of Optical Amplifiers, Intech, 2015
[22] Randhawa R., Singh S., Sohal J.S., Kaler R.S., Wavelength converter using semiconductor optical amplifier Mach-Zehnder interferometer based on XPM at 40 Gb/s for future transport networks, Fibe. Integr. Opti., 2009, 28(2), 154-69.
[23] Contestabile G., Yoshida Y., Maruta A., Kitayama K., Coherent wavelength conversion in a quantumdot SOA, Phot. Techn. Lett., IEEE, 2013, 25(9), 791-794.
[24] Qin J., Wang H., Wang D., Zhang M., Ji Y., Lu G.W., QPSK wavelength multicasting based on four-wave mixing in semiconductor opti- cal amplifier, Chin. Opt. Letters., 2014, 12(11), 110601
[25] Qin J., Ji Y.,Wang H.,Wang D., Zhang M., Lu G.W., Multichannel wavelength multicasting for two QPSK signals based on FWMin SOA, Chin. Opt. Lett., 2015, 13(1), 010601.
[26] Thomas A., Simultaneous Wavelength Preserving and Wavelength Converting Regeneration of NRZ DPSK Signal Using FWM inSOA, IJIRS-ET, 2014, 3(1), 550-557.
[27] Awang NA, AhmadH, Latif AA, Zulkifli MZ, Harun SW., Four-wave mixing in dual wavelength fiber laser utilizing SOA for wavelength conversion, Optik-Int. Jour. Lig. and Elect Opti., 2011, 122(9), 754-757.
[28] Guo L.Q., Connelly M.J., A novel approach to all-optical wavelength conversionby utilizing areflective semiconductor optical amplifier in a co-propagation scheme, Opti. Communi., 2008, 281(17), 4470-4473.
[29] Chung H.S., Inohara R., Nishimura K., Usami M., All-optical multiwavelength conversion of 10 Gbit/s NRZ/RZ signals based on SOA-MZI for WDM multicasting, Electr. Lett., 2005, 41(7), 432-433.
[30] Yan N., Monroy I.T., Jung H.D., Koonen T., Teixeira A., Silveira T., Optical multicast technologies by multi-wavelength conversion for optical routers, (Nov 27, 2006), International Conference on Communication Technology, IEEE, 2006, 1-4.
[31] Raz O., Herrera J., Calabretta N., Tangdiongga E., Anantathanasarn S., Nötzel R., Dorren H.J., Non-inverted multiple wavelength con- verter at 40 Gbit/s using 1550 nm quantum dot SOA, Elect Letters, 2007, 44(16), 988-989.
[32] Ab-rahman M.S., Swedan A.A., Optical Channel Capacity Upgrade Based on Multi-wavelength Conversion XGM Using Semiconductor Optical Amplifier for Access Networks, Inter. Jour. of Optics, 2017, 2017, 8
[33] Ab-rahman M.S., Swedan A.A., Semiconductor Optical Amplifier for Optical Channel Capacity Improvement Based on Cross-Phase Modulation, 4th International Conference on Communication and Computer Engineering, (April-2017), Penang, Malaysia, (in press)
[34] Connelly M.J., Wideband Semiconductor Optical Amplifier Steady-State Numerical Model, 2001, 37(3), 439-447.
[35] Connelly M.J., Semiconductor optical amplifiers, Springer Science & Business Media, 2007, 69-94,.
[36] Tang X., Kim N.Y., Cartledge J.C., Noise transfer characteristics in a semiconductor optical amplifier with application to wavelength conversion based on a delay interferometer, Jour. Ligh. Technology, 2008, 26(12), 1715-1721.
[37] Ribeiro N.S., Cavacalcante A.L., Gallep C.M., Conforti E., Optical amplitude modulation extinction by a deep saturated ultra-long semiconductor optical amplifier, 2010, Opti. express, 18(26), 27298-27305.
[38] Ribeiro D.O., Pontes M.J., Giraldi M.T., Characterization of all-optical wavelength conversion by cross-gain modulation of ASE on a SOA, MTT-S International Conference, Microwave and Optoelectronics, IEEE, 2005, 218-222.